

Progress in Nuclear Energy
Manuscript Draft

Manuscript Number: PNUCENE-D-17-00589

Title: Thermal-hydraulic noise analysis of a VVER-1000 reactor with nanofluid as coolant

Article Type: Research Paper

Keywords: Thermohydraulic noise,
Pressurized water reactor,
Nanofluid,
Frequency

- A model is developed for calculating the effects of a fluctuation in coolant temperature or coolant velocity at the inlet of a fuel assembly in VVER-1000 reactor with nanofluid as coolant.
- Code validation is made through of the applied model and previous studies performed with porous media approach, showed a good agreement.
- Calculations showed that, the temperature fluctuation at coolant inlet will propagate linearly through the coolant channel and with increment in nanoparticles mass fraction the fluctuations in axial coolant temperature and velocity will be reduced.

Thermal-hydraulic noise analysis of a VVER-1000 reactor with nanofluid as coolant

1 Reza Nourollahi^a, Mohammad Hossein Esteki^a, Golamreza Jahanfarnia^b
2
3
4
5
6

^aDepartment of Nuclear Engineering, University of Isfahan, Hezarjarib Avenue, P.O. Box 81746-73441, Isfahan,
Iran

^bDepartment of Nuclear Engineering, Science and Research Branch, Islamic Azad University, Tehran, Iran

Abstract

The noise issue, especially in industrial scale systems including nuclear power plants, there have been always an interesting subject in system stability analysis. Following the early studies about applying a water base Al_2O_3 nanofluid as coolant in VVER-1000 reactor, in this paper the effects of a fluctuation in coolant temperature or coolant velocity at the inlet of a fuel assembly was investigated by using a Fourier transformed conservation equation (mass, momentum and energy) in frequency space. The transformed equations were discretized with finite volume method and numerically solved. Thermodynamic properties of nanofluid was evaluated by adding new subroutines to IPAWS IF97 steam table libraries. The comparison between the achieved results of the applied model and previous studies performed with porous media approach, showed a good agreement. Thermal-hydraulic effects of nanofluid on noise fluctuations were calculated based on different concentrations of Al_2O_3 nanoparticle and noise frequencies. Calculations showed that any increment in nanoparticles mass fraction will result in reduction of fluctuations in coolant temperature and velocity.

Keywords

Thermal-hydraulics noise, Pressurizer water reactor, Nanofluid, Frequency.

1. Introduction

The most important intrinsic limitation consists in the relatively low thermal conductivity of conventional fluids. For instance, water has the highest thermal conductivity among all the fluids most commonly used today, although it is only equal to 0.6 W/m.K at room temperature, and that is several orders of magnitude lower than the thermal conductivity of metals, solid metal oxides (Mauro Lomascolo et al., 2015). Therefore, it would be logical to combine the conventional coolants with high thermal conductivity metals in order to upgrade the coolant properties.

(The literature review of steady stated analysis of applying nanofluids in a pressurized water reactor.) Choi, S.U.S (1995) shows that an increase in nanoparticles concentration will result in an increase in coolant outlet temperature, convection heat transfer coefficient and overall coolant pressure drop; while adding the nanoparticles into the coolant will reduce the neutron flux and neutronic efficiency.

Temperature or density fluctuations, as well as charging primary pumps fluctuations were investigated first in the early 1970s (Kosály and Williams, 1971). In these early works, a lumped model of thermal-hydraulics calculations (full of simplifying approximations) was used, which cannot show the exact behavior of the real systems.

According to Katona, et al. (1982), an inlet temperature change in light water reactors could lead to a local neutron flux fluctuation followed by coolant density (and neutron cross section) fluctuation. Also, it was reported that three sources of coolant temperature fluctuation can be identified AS :

1. Inlet temperature fluctuations;
2. Coolant velocity fluctuations, and ;
3. Power fluctuations.

Furthermore, Larsson and Demazière (2012) developed a coupled neutronics and thermalhydraulics tool for calculating fluctuations in PWRs. However, they have made some simplifying approximations in the thermal-hydraulics section (such as one-dimensional flow along the axial direction, uniform pressure and neglecting the effect of stresses, neglecting the fluctuations of the heat transfer coefficient, and a lumped model of the heat transfer from the fuel to the coolant), which have been improved partially by Demazière et al. (2014). For instance, the pressure distribution has been taken into account and a simple model for two-phase flow has been considered. However, the tool still contains some other approximations in the thermal-hydraulics section. Moreover, their developed computational tool cannot be used for modeling the propagation noise in VVER-1000 type pressurized water reactors.

More recently, a computational code (SHC-Noise) has been developed for the thermal-hydraulic fluctuations in PWR fuel assemblies, without the aforementioned simplifying assumptions (Malmir and Vosoughi, 2015a). Later on, Valkó, J., (1992) investigated PWR in-core generated temperature fluctuations versus fluctuations already present at inlet studied a special experiment to measure temperature fluctuation in a number of axial positions inside a fuel assembly.

The thermal hydraulic analysis of nuclear reactors and its noise response to any possible boundary condition fluctuations (such as mass flow rate fluctuations caused by pump), have been always one of the main issues in reactor core design. Following the previous literature studies on applying water-based nanofluid as coolant in PWRs, in this study, it is desired to develop a frequency-based calculation method to investigate the thermal hydraulic aspect of coolant fluctuations (inlet temperature and velocity). For this purpose, conservation equations of mass, momentum and energy were converted into frequency space and thermodynamic properties of coolant were evaluated by developing the IPAWS-IF97 (Wagner and Kretzschmar, 2008) for water based Al_2O_3 nanofluids. Finally, a computer code was developed to simulate fluctuations of reactor coolant.

Al_2O_3

Nomenclature

ρ	Density (kg/m^3)
v	Velocity (m/s)
T	Time (s)
P	Pressure ($\text{kg}/\text{m.s}^2$)
g	Acceleration of gravity (m/s^2)
h	Specific enthalpy (J/kg)
q	Heat power (W)
q''	Heat flux (W/m^2)
q'''	Volumetric heat power (W/m^3)
C_p	Specific heat capacity ($\text{J}/\text{kg.}^\circ\text{C}$)
T	Temperature ($^\circ\text{C}$)
k	Heat conductivity ($\text{W}/\text{m.}^\circ\text{C}$)
μ	Dynamic viscosity ($\text{kg}/\text{m.s}$)
h_s	Heat transfer coefficient ($\text{W}/\text{m}^2.^\circ\text{C}$)
D_e	Equivalent hydraulic diameter (m)
P_w	Wetted perimeter (m)
P_h	Heated perimeter (m)
Re	Reynolds number, $\rho v D_e / \mu$
Pr	Prandtl number, $\mu C_p / k$
Nu	Nusselt number, $h_s D_e / k$
R	Radius (m)
ω	Angular frequency (rad/s)
V	Volume (m^3)
f	Darcy (Moody) friction factor

Subscripts

m	Coolant
f	Fuel
c	Clad
g	Gap
co	Cladding outer surface
ci	Cladding inner surface
fo	Fuel outer surface
fi	Fuel inner surface
ϕ	. Nanoparticles concentration
M	. Mass
nf	Nanofluid
bf	. Basefluid
np	Nanoparticle

NOT
SUBSCRIPT?

Operators

$\langle \rangle$	Volume averaging operator
$\{ \}$	Surface averaging operator

1
2
3
4
5
6
7
8
9
10
11
12
13
14
15
16
17
18
19
20
21
22
23
24
25
26
27
28
29
30
31
32
33
34
35
36
37
38
39
40
41
42
43
44
45
46
47
48
49
50
51
52
53
54
55
56
57
58
59
60
61
62
63
64
65

2. Methods And Material

2.1 Thermal-hydraulic Equations

In order to derive the single-phase thermal–hydraulics noise equations, one starts the mass, momentum and energy conservation laws for the single-phase coolant as follows (Todreas and Kazimi, 2001):

$$\frac{\partial}{\partial t} \rho_m(r, t) + \nabla \cdot [\vec{v}_m(r, t) \rho_m(r, t)] = 0 \quad (1)$$

$$\frac{\partial}{\partial t} [\rho_m(r, t) \vec{v}_m(r, t)] = -\nabla \cdot (\bar{\tau} - P\bar{I}) + \rho_m(r, t) \vec{g} + \nabla \cdot [\rho_m(r, t) \vec{v}_m(r, t) \vec{v}_m(r, t)] \quad (2)$$

$$\frac{\partial}{\partial t} [\rho_m(r, t) h_m(r, t) - p] + \nabla \cdot [\rho_m(r, t) h_m(r, t) \vec{v}_m(r, t)] = -\nabla \cdot q(r, t) + \vec{v}_m \cdot [\nabla \cdot (\bar{\tau} - P\bar{I})] \quad (3)$$

These equations are solved in an iterative manner to get the pressure, temperature and velocity distribution of the moderator in all nodes of the reactor. *TUC*

Where $\nabla \cdot \bar{\tau}$ denotes the internal stress force and \bar{I} is identity tensor. Furthermore, $\vec{v}_m \vec{v}_m$ is a dyadic product of all the velocity components, moreover, the convection heat flux q'' can be expressed:

$$q'' = h_{sm}(T_{co} - T_m) \quad (4)$$

The internal stress force ($\nabla \cdot \bar{\tau}$) is given as follows:

$$\nabla \cdot \bar{\tau} = -\frac{f}{2D_e} (\rho_m \vec{v}_m^2) \quad (5)$$

Assuming a one-dimensional upward flow along a vertical single heated channel. The energy equation describing the temperature distribution in a PWR fuel element (which is assumed to be an incompressible material with negligible thermal expansion) can be written as (Todreas and Kazimi, 2001):

$$\rho_f(T_f) c_f(T_f) \frac{\partial}{\partial t} T_f(r, t) = -\nabla \cdot q''(r, t) + q''(r, t) \rightarrow \text{SHOULDN'T IT BE } C_p f ? \quad (6)$$

Fourier's law of conduction, can be rewritten as:

$$\rho_f(T_f) c_f(T_f) \frac{\partial}{\partial t} T_f(r, t) = -\nabla \cdot [k_f(T_f) \nabla T_f(r, t)] + q(r, t) \text{ DISCRETISE} \quad (7)$$

In order to calculate the thermal–hydraulics fluctuations in a pressurized water reactor, the finite volume method (FVM) was applied to discrete the conservation equations. The area-average quantities will be denoted as (Nakamura, 1977; Murthy 2002):

$$\{x_m\} = \frac{1}{A_m} \int x_m ds \quad (8)$$

And volume-averaged quantities denoted as:

$$\langle x_m \rangle = \frac{1}{V_m} \int x_m dV \quad (9)$$

With A_m and V_m being the cross-sectional area and volume of a node, respectively, at a given elevation.

To solve the system of equations, a relation between the area-averaged values and the volume-averaged values must be established. It is here assumed that:

$$\langle x_m \rangle = \frac{\{x_m\}^+ + \{x_m\}^-}{2} \quad (10)$$

And the equations are solved at the faces in between the nodes and the node average is constructed afterwards using the relation in Equation (10).

The integrated thermal-hydraulics equations are given by:

$$\frac{\partial}{\partial t} \int_{V_{m_{nf}}} \rho_{m_{nf}}(r, t) dV + \int_{V_{m_{nf}}} \nabla \cdot [\vec{v}_{m_{nf}}(r, t) \rho_{m_{nf}}(r, t)] dV = 0 \quad (11)$$

$$\begin{aligned} & \frac{\partial}{\partial t} \int_{V_{m_{nf}}} [\rho_{m_{nf}}(r, t) \vec{v}_{m_{nf}}(r, t)] dV + \int_{V_{m_{nf}}} \nabla \cdot [\rho_{m_{nf}}(r, t) \vec{v}_{m_{nf}}(r, t) \vec{v}_{m_{nf}}(r, t)] dV = \\ & + \int_{V_{m_{nf}}} \nabla \cdot (\bar{\tau} - P \bar{I}) dV + \int_{V_{m_{nf}}} \rho_{m_{nf}}(r, t) \vec{g} dV \end{aligned} \quad (12)$$

$$\begin{aligned} & \frac{\partial}{\partial t} \int_{V_{m_{nf}}} [\rho_{m_{nf}}(r, t) h_{m_{nf}}(r, t) - p] dV + \int_{V_{m_{nf}}} \nabla \cdot [\rho_{m_{nf}}(r, t) h_{m_{nf}}(r, t) \vec{v}_{m_{nf}}(r, t)] dV \\ & = - \int_{V_{m_{nf}}} \nabla \cdot q(r, t) dV + \int_{V_{m_{nf}}} \vec{v}_{m_{nf}} \cdot [\nabla \cdot (\bar{\tau} - P \bar{I})] dV \end{aligned} \quad (13)$$

Pressing all the time-dependent terms in the transient conservation equation as:

$$X(r, t) = X_0(r) + \delta X(r, t) \quad (14)$$

$X_0(r)$, $\delta X(r, t)$ in Eqs.(14) are parts steady state and fluctuations.

For the following thermodynamic properties:

$$\rho_{m_{nf}} = \rho_{m_{nf,o}} + \delta \rho_{m_{nf}} \quad (15)$$

$$h_{m_{nf}} = h_{m_{nf,o}} + \delta h_{m_{nf}} \quad (16)$$

$$P_{m_{nf}} = P_{m_{nf,o}} + \delta P_{m_{nf}} \quad (17)$$

$$v_{m_{nf}} = v_{m_{nf,o}} + \delta v_{m_{nf}} \quad (18)$$

And removing all the second-order terms, then removing the steady-state and finally performing a **temporal Fourier transform** on remaining terms as:

$$\delta X(r, \omega) = \int_{-\infty}^{+\infty} \delta X(r, t) \exp(-i\omega t) dt \quad (19)$$

lead to the thermal-hydraulics noise equations as follows:

$$\int_{V_{m_n}} i\omega \delta\rho_{m_n} dV + \int_{V_{m_n}} \nabla \cdot (\rho_{m_n} \delta \vec{v}_{m_n} + \vec{v}_{m_n} \delta \rho_{m_n}) dV = 0 \quad (20)$$

$$\begin{aligned} & \int_{V_{m_n}} i\omega (\rho_{m_n} \delta \vec{v}_{m_n} + \vec{v}_{m_n} \delta \rho_{m_n}) dV + \int_{V_{m_n}} \nabla \cdot (\vec{v}_{m_n} \vec{v}_{m_n} \delta \rho_{m_n} + \\ & 2\rho_{m_n} \vec{v}_{m_n} \delta \vec{v}_{m_n}) dV = \int_{V_m} \nabla \cdot (\bar{\delta\tau} - \delta P_{m_n} \bar{I}) dV \end{aligned} \quad (21)$$

$$\begin{aligned} & \int_{V_{m_n}} i\omega (\rho_{m_n} \delta h_{m_n} + h_{m_n} \delta \rho_{m_n} - \delta P) dV + \int_{V_{m_n}} \nabla \cdot (\rho_{m_n} h_{m_n} \delta \vec{v}_{m_n} + \\ & \rho_{m_n} \vec{v}_{m_n} \delta h_{m_n} + h_{m_n} \vec{v}_{m_n} \delta \rho_{m_n}) dV = \int_{V_{m_n}} -\nabla \cdot \bar{\delta q} dV + \int_{V_{m_n}} \vec{v}_{m_n} \cdot [\nabla \cdot (\bar{\delta\tau} - \bar{I})] dV + \\ & \int_{V_{m_n}} \nabla \cdot (\bar{\delta\tau}_o - P_o \bar{I}) \cdot \delta \vec{v}_{m_n} dV \end{aligned} \quad (22)$$

By using finite volume method based on Eqs.(8) and (9), Eqs.(20), (21) and (22) can be discretized into Thermal-hydraulic noise equations nanofluid coolant:

Velocity:

$$\begin{aligned} & \left\{ \rho_{m_n} \right\}^{j+\frac{1}{2}} \left\{ \delta v_{m_n} \right\}^{j+\frac{1}{2}} = \left(-\frac{i\omega \Delta z}{2} - \left\{ v_{m_n} \right\}^{j+\frac{1}{2}} \right) \left\{ \delta \rho_{m_n} \right\}^{j+\frac{1}{2}} + \left(-\frac{i\omega \Delta z}{2} + \left\{ v_{m_n} \right\}^{j+\frac{1}{2}} \right) \left\{ \delta \rho_{m_n} \right\}^{j-\frac{1}{2}} + \\ & \left(\left\{ \rho_{m_n} \right\}^{j-\frac{1}{2}} \right) \left\{ \delta v_{m_n} \right\}^{j-\frac{1}{2}} \end{aligned} \quad (23)$$

Pressure:

$$\begin{aligned} & \left\{ \delta p_{m_n} \right\}^{j+\frac{1}{2}} = \left\{ \delta p_{m_n} \right\}^{j-\frac{1}{2}} + \left\{ \delta v_{m_n} \right\}^{j+\frac{1}{2}} \left(-\frac{1}{2} i\omega \Delta z \langle \rho_{m_n} \rangle^j - 2 \left\{ \rho_{m_n} \right\}^{j+\frac{1}{2}} \left\{ v_{m_n} \right\}^{j+\frac{1}{2}} - \right. \\ & \left. \frac{1}{2D_e} \langle f_o \rangle^j \langle \rho_{m_n} \rangle^j \langle v_{m_n} \rangle^j \Delta z \right) + \left\{ \delta v_{m_n} \right\}^{j-\frac{1}{2}} \left(-\frac{1}{2} i\omega \Delta z \langle \rho_{m_n} \rangle^j + 2 \left\{ \rho_{m_n} \right\}^{j+\frac{1}{2}} \left\{ v_{m_n} \right\}^{j+\frac{1}{2}} - \right. \\ & \left. \frac{1}{2D_e} \langle f_o \rangle^j \langle \rho_{m_n} \rangle^j \langle v_{m_n} \rangle^j \Delta z + \left\{ \delta \rho_{m_n} \right\}^{j+\frac{1}{2}} \left(-\frac{1}{2} i\omega \Delta z \langle v_{m_n} \rangle^j - \langle v^2 \rangle_{m_n}^{j+\frac{1}{2}} - \right. \right. \\ & \left. \left. \frac{1}{2} \langle f_o \rangle^j \langle v^2 \rangle_{m_n}^{j+\frac{1}{2}} \Delta z - \frac{1}{2} g \Delta z \right) + \left\{ \delta \rho_{m_n} \right\}^{j-\frac{1}{2}} \left(-\frac{1}{2} i\omega \Delta z \langle v_{m_n} \rangle^j + \langle v^2 \rangle_{m_n}^{j+\frac{1}{2}} - \right. \right. \\ & \left. \left. \frac{1}{2} \langle f_o \rangle^j \langle v^2 \rangle_{m_n}^{j+\frac{1}{2}} \Delta z + \frac{1}{2} g \Delta z \right) \right) \end{aligned} \quad (24)$$

Enthalpy:

$$\begin{aligned}
& \left\{ \delta h_{m_{nf}} \right\}^{j+\frac{1}{2}} \times \left(\frac{1}{2} i \omega \Delta z \langle \rho_{m_{nf},o} \rangle^j + \left\{ \rho_{m_{nf},o} \right\}^{j+\frac{1}{2}} \left\{ v_{m_{nf},o} \right\}^{j+\frac{1}{2}} \right) \\
&= \left\{ \delta h_{m_{nf}} \right\}^{j-\frac{1}{2}} \times \left(\frac{1}{2} i \omega \Delta z \langle \rho_{m_{nf},o} \rangle^j + \left\{ \rho_{m_{nf},o} \right\}^{j-\frac{1}{2}} \left\{ v_{m_{nf},o} \right\}^{j-\frac{1}{2}} \right) \\
&+ \left\{ \delta p_{m_{nf}} \right\}^{j+\frac{1}{2}} \left(\frac{1}{2} i \omega \Delta z - \langle v_{m_{nf},o} \rangle^j \right) + \left\{ \delta p_{m_{nf}} \right\}^{j-\frac{1}{2}} \left(\frac{1}{2} i \omega \Delta z + \langle v_{m_{nf},o} \rangle^j \right) \\
&+ \left\{ \delta v_{m_{nf}} \right\}^{j+\frac{1}{2}} \left(- \left\{ \rho_{m_{nf},o} \right\}^{j+\frac{1}{2}} \left\{ h_{m_{nf},o} \right\}^{j+\frac{1}{2}} \right. \\
&\quad \left. + \frac{1}{2} \left[\left\{ p_{m_{nf},o} \right\}^{j+\frac{1}{2}} - \left\{ p_{m_{nf},o} \right\}^{j-\frac{1}{2}} + \frac{3 \Delta z}{2 D_e} \langle f_o \rangle^j \langle v^2 m_{nf,o} \rangle^j \langle \rho_{m_{nf},o} \rangle^j \right] \right) \\
&+ \left\{ \delta v_{m_{nf}} \right\}^{j-\frac{1}{2}} \left(+ \left\{ \rho_{m_{nf},o} \right\}^{j+\frac{1}{2}} \left\{ h_{m_{nf},o} \right\}^{j+\frac{1}{2}} \right. \\
&\quad \left. + \frac{1}{2} \left[- \left\{ p_{m_{nf},o} \right\}^{j+\frac{1}{2}} + \left\{ p_{m_{nf},o} \right\}^{j-\frac{1}{2}} + \frac{3 \Delta z}{2 D_e} \langle f_o \rangle^j \langle v^2 m_{nf,o} \rangle^j \langle \rho_{m_{nf},o} \rangle^j \right] \right) \\
&+ \left\{ \delta \rho_{m_{nf}} \right\}^{j+\frac{1}{2}} \left(- \left\{ v_{m_{nf},o} \right\}^{j+\frac{1}{2}} \left\{ h_{m_{nf},o} \right\}^{j+\frac{1}{2}} \right. \\
&\quad \left. - \frac{1}{2} i \Delta z \left[\omega \langle h_{m_{nf},o} \rangle^j + \frac{i}{2 D_e} \langle f_o \rangle^j \langle v^3 m_{nf,o} \rangle^j \right] \right) \\
&+ \left\{ \delta \rho_{m_{nf}} \right\}^{j-\frac{1}{2}} \left(+ \left\{ v_{m_{nf},o} \right\}^{j+\frac{1}{2}} \left\{ h_{m_{nf},o} \right\}^{j+\frac{1}{2}} \right. \\
&\quad \left. - \frac{1}{2} i \Delta z \left[\omega \langle h_{m_{nf},o} \rangle^j + \frac{i}{2 D_e} \langle f_o \rangle^j \langle v^3 m_{nf,o} \rangle^j \right] \right) + \frac{P_h \Delta z}{A_m} \langle q''' \rangle^j \\
&+ \frac{\Delta z}{2 D_e} \langle \rho_{m_{nf},o} \rangle^j \langle \delta f \rangle^j \langle v^3 m_{nf,o} \rangle^j
\end{aligned} \tag{25}$$

2.2 Fuel rod noise equations

The energy equation describing the temperature distribution in a PWR fuel element (which is assumed to be an incompressible material with negligible thermal expansion) can be written as (Todreas and Kazimi, 2001):

$$\rho c_p \frac{\partial T}{\partial t} = -\nabla \cdot \bar{q'''} + q''' \tag{26}$$

with the fluctuations of the convection heat flux ($\delta \bar{q''}$) as:

$$\delta \bar{q''} = h_{sm_{nf,o}} (\delta T_{co} - \delta T_m) + \delta h_{sm_{nf,o}} (T_{co,o} - T_{m,o}) \tag{27}$$

and the energy fluctuations equation for the fuel, gap and cladding as:

$$i\omega\rho C_p \delta T = -\nabla \cdot \vec{\delta q}'' + \delta q''' \quad (28)$$

from which the fluctuations of the volumetric heat power term ($\delta q'''$) must be excluded for the thermal-hydraulics noise calculations in the gap and cladding where $\nabla \cdot \bar{\tau}$ denotes the internal stress force and \bar{I} is the identify tensor. Furthermore, $v_m v_m$ is a dyadic product of all the velocity components. Moreover, the heat flux (q''_0) can be expressed as:

$$q''_0 = h_{sm_{nf,o}} (T_{co,o} - T_{m,o}) \quad (29)$$

Equations of Temperature fluctuation in fuel rods as:

Clad Outside Temperature:

$$\langle \delta T_{co} \rangle^j = \langle \delta T_m \rangle^j + \frac{1}{\langle h_{sm_{nf,o}} \rangle^j} \langle \delta q'' \rangle^j - \frac{\langle \delta h_{sm_{nf}} \rangle^j}{\langle h_{sm_{nf,o}} \rangle^j} \quad (30)$$

Clad Inside Temperature:

$$\left(\frac{i\omega \rho_g c_{pg} (r_{ci}^2 - r_{fo}^2)}{4} + \langle h_{sg} \rangle^j r_{fo} \right) \langle \delta T_{ci} \rangle^j = \left(-\frac{i\omega \rho_g c_{pg} (r_{ci}^2 - r_{fo}^2)}{4} + \langle h_{sg} \rangle^j r_{fo} \right) \langle \delta T_{fo} \rangle^j + \frac{q}{2\pi\Delta z} \quad (31)$$

Fuel Pellet Temperature:

$$\begin{aligned} & \left(-\{k_f\}^{i+\frac{1}{2}} \cdot r_{i+\frac{1}{2}} \langle \delta T_f \rangle^{i+1} + \left(-\{k_f\}^{i+\frac{1}{2}} \cdot r_{i+\frac{1}{2}} - \{k_f\}^{i-\frac{1}{2}} \cdot r_{i-\frac{1}{2}} \right) \langle \delta T_f \rangle^i + \left(-\{k_f\}^{i-\frac{1}{2}} \cdot r_{i-\frac{1}{2}} \right) \langle \delta T_f \rangle^{i-1} + \right. \\ & \left. \left(i\omega \langle \rho_f \rangle^i \langle c_{pf} \rangle^i \frac{\Delta r}{2} \left(r_{i+\frac{1}{2}}^2 - r_{i-\frac{1}{2}}^2 \right) \right) \langle \delta T_f \rangle^i = (\delta q'') \frac{\Delta r}{2} \left(r_{i+\frac{1}{2}}^2 - r_{i-\frac{1}{2}}^2 \right) \right) \quad (32) \end{aligned}$$

2.3 Nanofluid thermodynamic properties

Consider a homogeneous colloid made of a base fluid and nanoparticles, called nanofluid (J. Buongiorno, 2005), in an arbitrary control volume, V (see Figure 1). The *colloid* definition states that there is a specified number of nanoparticles per each molecule of base the fluid. According to (M.H.Rahimi et al., 2017) report, and regarding the definition of colloid, the *nanoparticle mass fraction* is constant through the heated channel, while due to variation of density, the *volume fraction* values changes:

$$\varphi_M = \frac{M_{np}}{M_{nf}} = \frac{N_{np} \cdot m_{np}}{N_{np} \cdot m_{np} + N_{bf} \cdot m_{bf}} = \text{constant} \quad (33)$$

$$\varphi_V = \frac{V_{np}}{V_{nf}} = \frac{\rho_{bf}}{\rho_{bf} + \rho_{np} \cdot \frac{(1-\varphi_M)}{\varphi_M}} \quad (34)$$

NOT CLEAR WHAT THESE VARIABLES

MEAN.

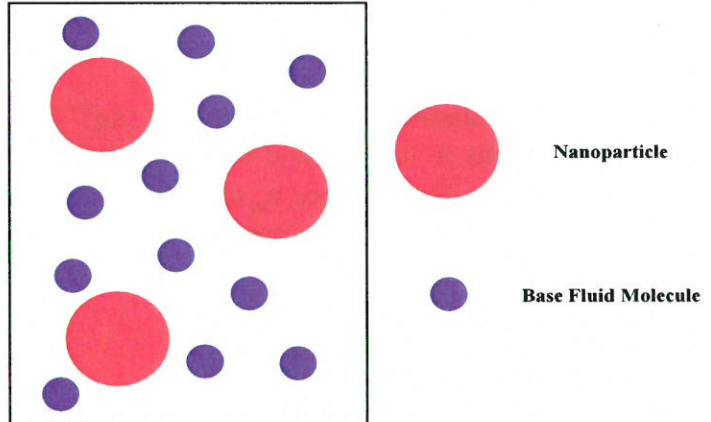


Fig. 1. Homogeneous Nanofluid in an arbitrary control volume.

As it was mentioned earlier, combining a nanoparticle with a base fluid will result in alteration of intrinsic properties of the base fluid, including Density (ρ), Specific Isobaric Heat capacity (C_p), Viscosity (μ), Thermal Conductivity (k_e). According to the literature review, there have been proposed two kind of correlations to evaluate the thermodynamic properties of nanofluid: a) theoretical correlations based on Brownian motion (Sheng-Qi Zhou and Rui Ni, 2008) and b) empirical correlations based on experimental studies (M. Ebrahimian and G.R. Ansarifar, 2016). Nanofluid density (ρ_{nf}) and specific heat capacity (C_{p-np}) are defined respectively as follows (Sheng-Qi Zhou and Rui Ni, 2008):

$$\rho_{nf} = \varphi_V \cdot \rho_{np} + (1 - \varphi_V) \cdot \rho_{bf} \quad (35)$$

$$C_{p-np} = \frac{\varphi_V \cdot (\rho \cdot C_p)_{np} + (1 - \varphi_V) \cdot (\rho \cdot C_p)_{bf}}{\varphi_V \cdot \rho_{np} + (1 - \varphi_V) \cdot \rho_{bf}} \quad (36)$$

G. Jahanfarnia et al. (?) reported, that due to a better neutronic properties of Al_2O_3 (low neutron absorption cross section) compared with other nanoparticles (Cu, TiO_2 , etc), utilization of this nanoparticle in nuclear reactors would be more reasonable. Ebrahimian and Ansarifar recommended the Masumi's correlation to evaluate the viscosity of water base Al_2O_3 nanofluids:

$$\mu_{nf} = \mu_{bf} \left(1 + \frac{\rho_{np} V_b d_{np}^2}{72 \cdot N \cdot \delta} \right) \quad (37)$$

In which, d_{np} , δ and V_b are nanoparticles diameter, average distance between two nanoparticles and Brownian velocity of nanoparticles, respectively:

$$\delta = \sqrt[3]{\frac{\pi}{6 \cdot \varphi_V}} d_{np} \quad (38)$$

$$V_b = \frac{1}{d_{np}} \sqrt{\frac{18 k_B T}{\pi \cdot \rho_{np} \cdot d_{np}}} \quad (39)$$

And N is a function of nanoparticle volume fraction which is calculated as follows:

$$N = (C_1 \varphi_V + C_2) d_{np} + C_3 \varphi_V + C_4 \quad (40)$$

$$C_1 = -1.133e^{-6}, C_2 = -2.771e^{-6}, C_3 = -9.0e^{-8}, C_4 = -3.93e^{-7} \quad (UNITS?) \quad (41)$$

The following correlation to calculate the thermal conductivity of water base AL_2O_3 nanofluids:

$$k_{e-\text{NanoFluid}} = k_{e-\text{BaseFluid}}(1 + 2.72\varphi_V + 4.97\varphi_V^2) \quad (42)$$

2.4. Boundary conditions

The assumed boundary condition (coolant inlet velocity, temperature, pressure and power distribution) are presented in figure [2], table [1].

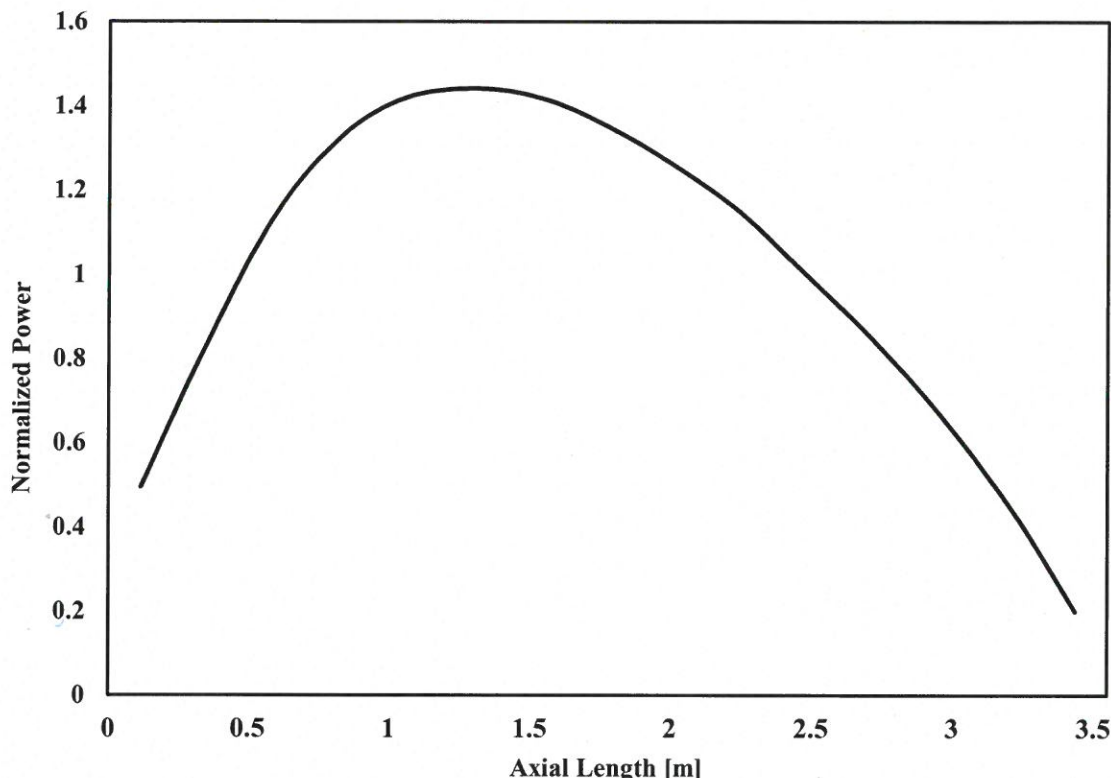


Fig. 2. Normalized axial Power distribution in the VVER-1000 reactor.

Table 1. Thermo-hydraulic boundary conditions of the simulation (AEOI, 2007).

Boundary Condition	Value
Average Coolant Inlet Velocity in core reactor	5.6 [m/s]
Core Outlet Pressure	157 [bar]
Flow rate through the reactor	84800 [m ³ /h]
Coolant temperature at the reactor inlet	291 [°C]
Coolant temperature at the reactor outlet	321 [°C]
Coolant enthalpy at the reactor inlet	1290 [°C]

Table 2. Input parameters for the case study of a typical VVER-1000 core (AEOI, 2007).

Parameter	Value
Reactor thermal power	3000 MW
Number of fuel assemblies (FAs)	163
Number of fuel rods in a FA	311
Number of non-fuel tubes in a FA	20
Pitch between FAs	23.6 cm
Pitch between fuel rods	1.27 cm
FA height	355 cm
Coolant temperature at the reactor inlet	291 °C
Coolant pressure at the core outlet	15.7 MPa
Coolant mass flux	4058 kg/m ² s
Cladding outside diameter	9.1 mm
Cladding inside diameter	7.73 mm
Fuel pellet outside diameter	7.57 mm
Fuel pellet outside diameter	1.50 mm

3. Calculations flowchart

3.1 Steady calculations

For steady state and transient conditions, thermal-hydraulic analysis in reactor core follows the procedure presented in figure 3 and 4, respectively. According to these flowcharts a computer code was developed and thermal-hydraulic parameters of core were calculated.

Code

→ MORE DETAILS ABOUT
* THE MODEL & ASSOCIATE
SOLUTION METHODS
~~SHOULD BE~~ SHOULD BE
CLEARLY DESCRIBED

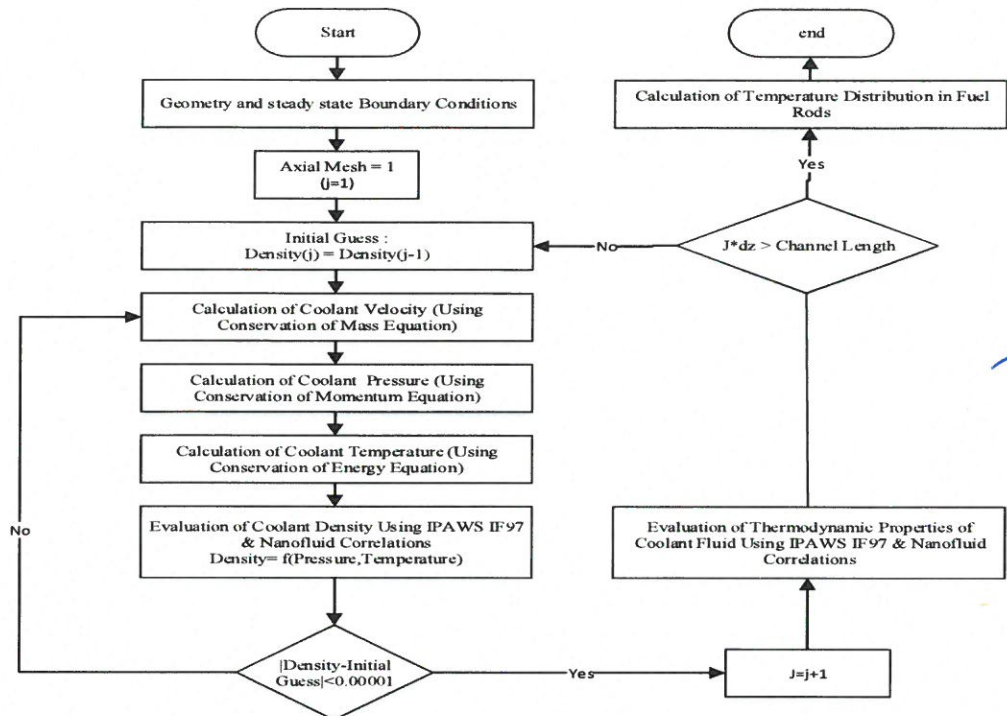


Fig. 3. The flowchart of the closed-loop steady-state calculations.

3.2 Noise calculations

SAME CONDITIONS AS IN *1!

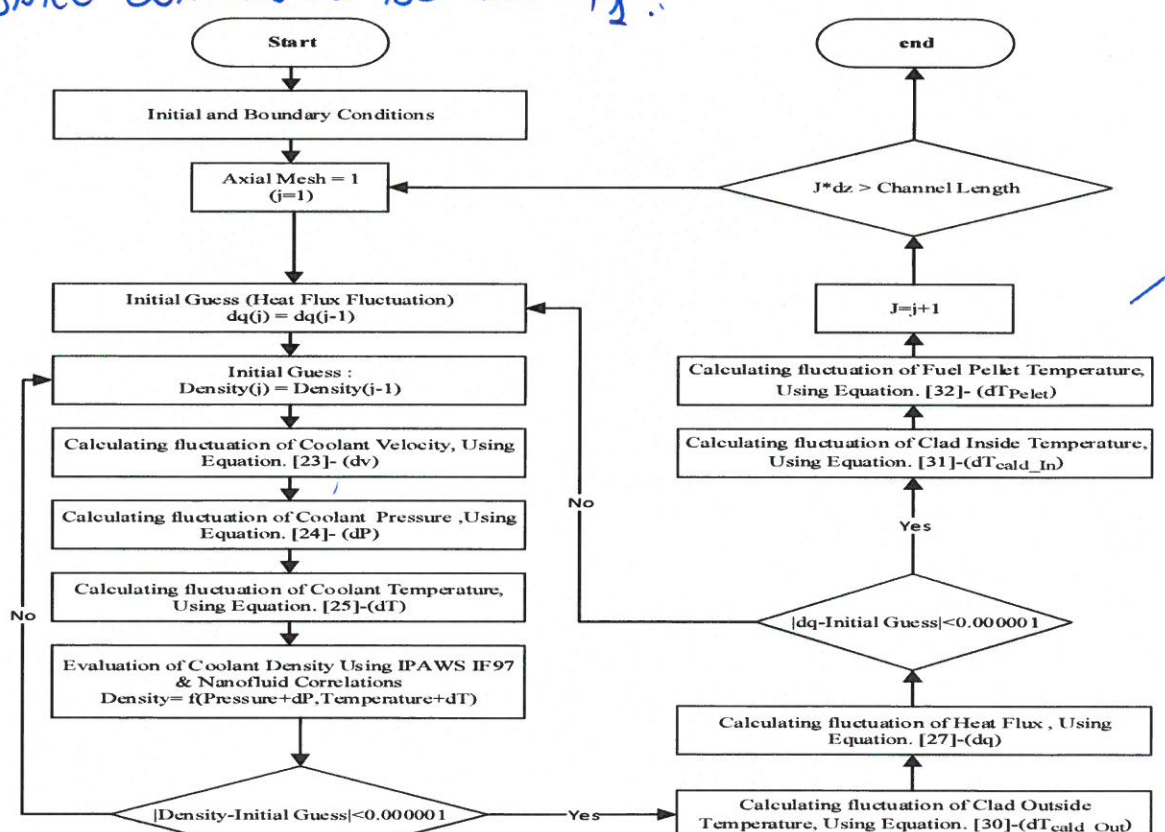


Fig. 4. The flowchart of the closed-loop noise calculations.

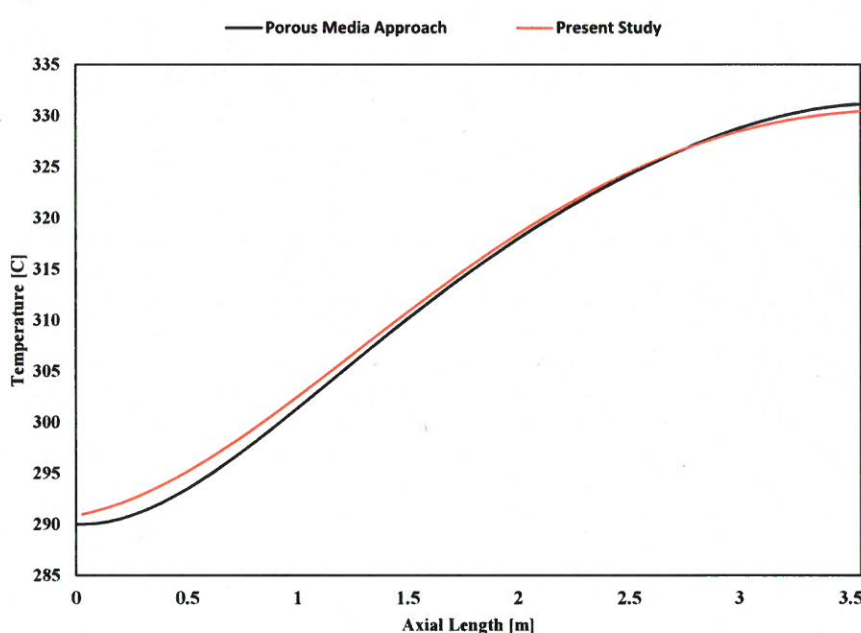
4. Results and Discussion

Calculations are performed in the hot channel of a typical VVER-1000 core with boundary conditions listed in Table [5], for different concentration of Al_2O_3 nanofluid ($\varphi_M = 1\%, 5\%, 10\%, 20\%$).

4.1 Steady state simulation

The coolant enters the fuel assemblies with average temperature 291 °C and removes the power generated in fuels rods through the reactor core. Axial normalized power generation in a typical VVER-1000 core reactor is shown in figure 5.

Figure 5 illustrate the coolant temperature along the hot fuel assembly length. The comparison between the results for present model and those reported by (M.H.Rahimi and G.Jahanfarnia, 2014) shows a good agreement.



IT SHOULD
BE GOOD TO
HAVE MORE
DETAILS ON
THE METHODS
USED FOR
COMPARISON.

Fig. 5. Variation of coolant temperature in hot fuel assembly.

It is well known that a temperature rise in reactor coolant will result in reduction of coolant density. Regarding to continuity equation, $(\rho Av)_{inlet} = (\rho Av)_{outlet}$, considering $A_{inlet} = A_{outlet}$, a reduction in coolant density will result in an increment in coolant velocity. The variation of coolant density and velocity are depicted in figure 6 and 7.

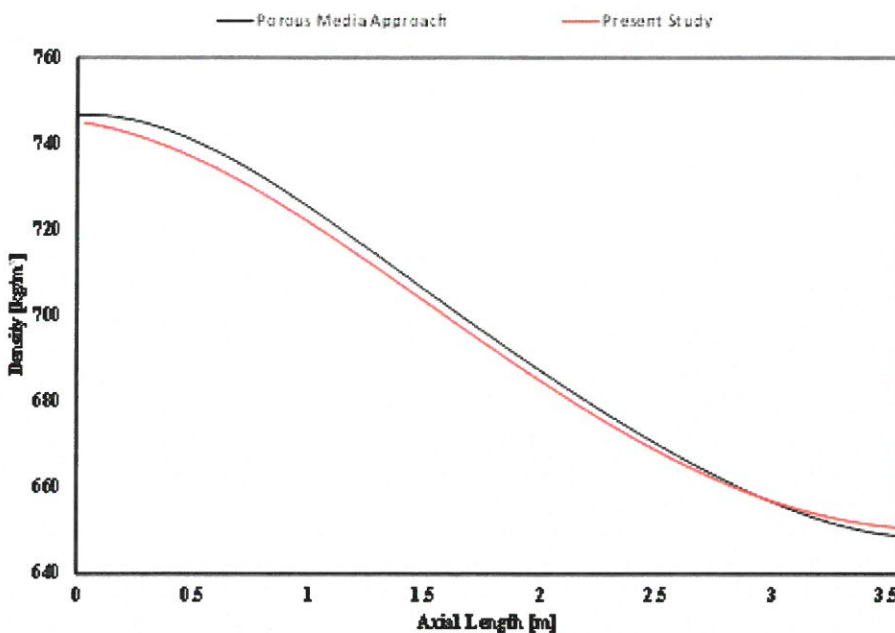


Fig. 6. Variation of coolant density in hot fuel assembly.

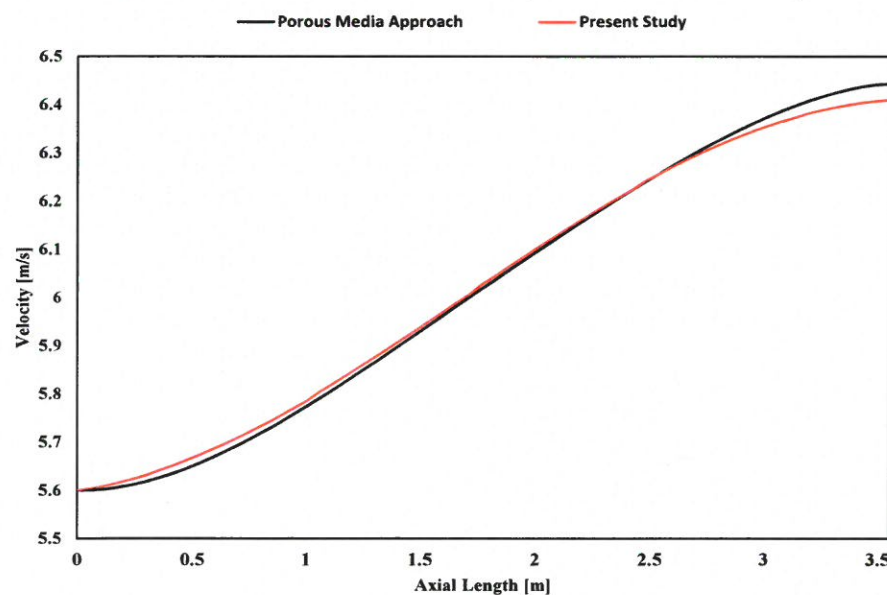


Fig. 7. Variation of coolant velocity in hot fuel assembly.

According to conservation equation of momentum [8], variation of pressure along the fuel assembly in steady states is due to coolant-fuel rods friction ($\Delta P_{\text{friction}}$) and abrupt flow area changes at grid spacers (ΔP_{form}). Figure 8 illustrates the variation of coolant pressure in the hot fuel assembly. As one can see, the pressure drop due to grid spacers play the major role in total coolant pressure drop.

role

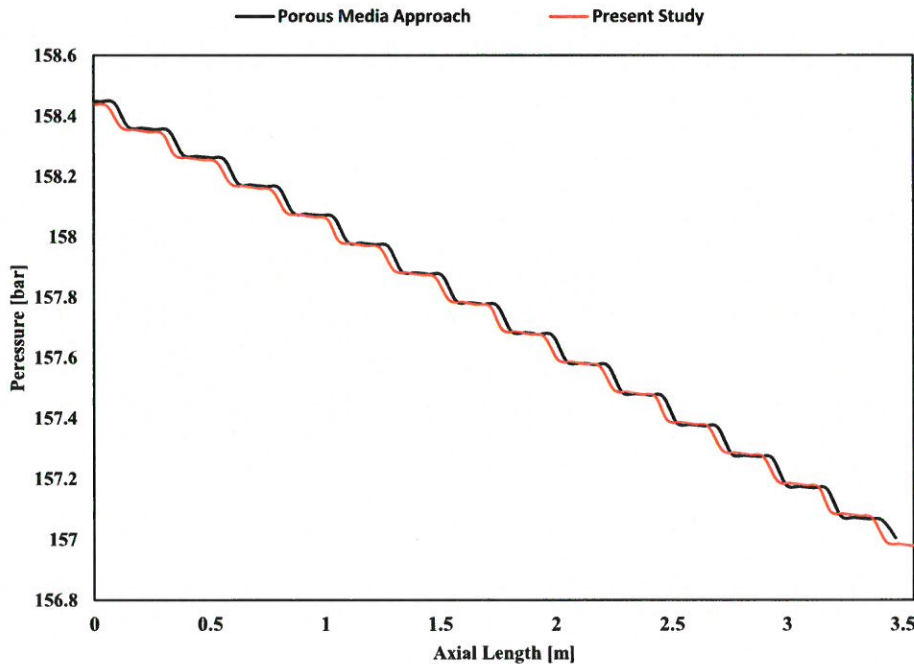


Fig. 8. Variation of coolant pressure in hot fuel assembly.

The most fascinating feature of a nanofluid compared with conventional coolants, which leads us to apply it in a high heat flux system, is the improvement of the heat transfer coefficient (HTC). The calculations show that the increment of nanoparticle mass fraction will result in an amplification in coolant HTC. Figure 9 illustrate the HTC of coolant in the reactor core.

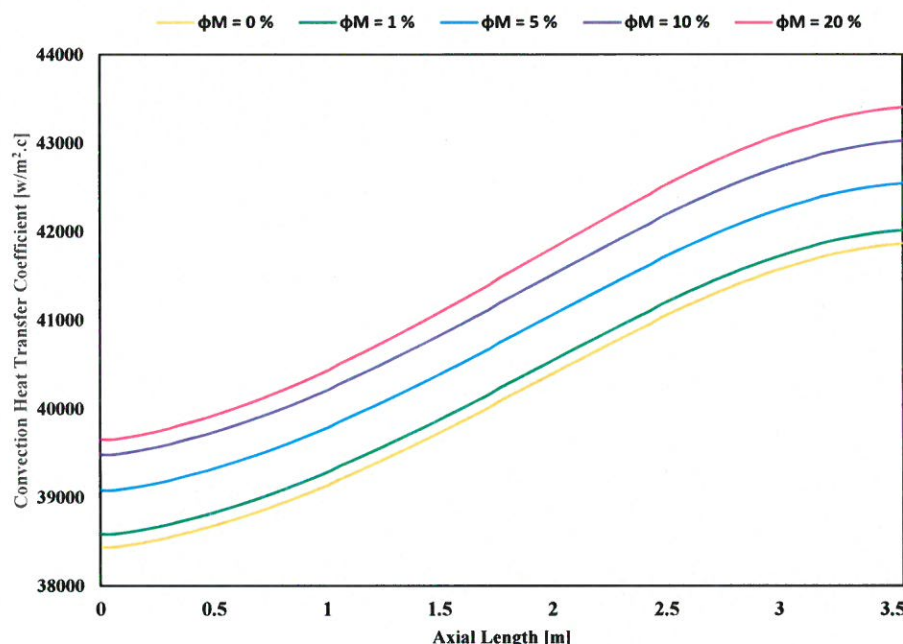


Fig. 9. Variation of convection heat transfer coefficient in hot fuel assembly with the different nanoparticle mass fraction.

4.2 Noise simulation

Thermal-hydraulic noise analysis was performed in a typical VVER-1000 reactor with water base Al_2O_3 nanofluid coolant, for two different transient scenarios: fluctuations in a) Coolant inlet temperature and b) Coolant inlet velocity ($f = 0.1$ and 1.0 Hz).

It is assumed that in the first scenario, the coolant inlet temperature fluctuates 0.4°C with the frequency equal to 0.1 Hz and 1.0 Hz. Figure 10 and 11 illustrate the fluctuation magnitude and phase over the hottest channel in reactor core for $f = 0.1$ Hz and 1.0 Hz, respectively. In both frequencies, any increase in nanofluid mass fraction will result in reduction of outlet temperature. It should be noted that, the maximum difference between inlet and outlet temperature fluctuation is $\sim 0.09^\circ\text{C}$ and fluctuations propagate linearly through the channel (See Figure 10-b and 11-b).

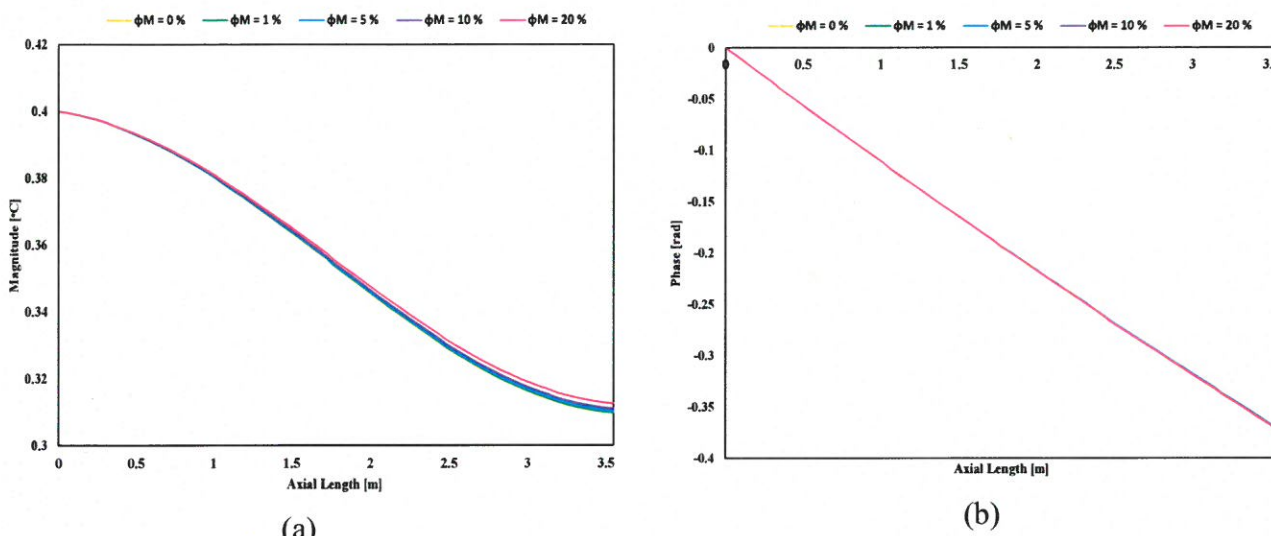


Fig. 10. F fluctuation of coolant temperature for different Al_2O_3 nanofluid mass fraction ((a) Magnitude, (b) Phase)-frequency = 0.1 Hz.

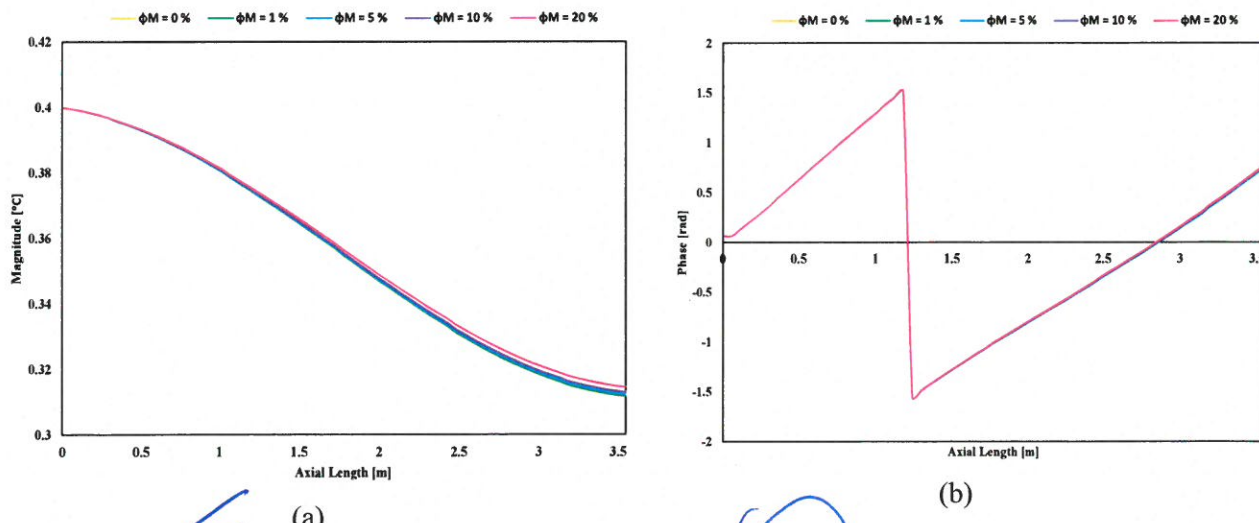


Fig. 11. F fluctuation of coolant temperature for different Al_2O_3 nanofluid mass fraction ((a) Magnitude, (b) Phase)-frequency = 1.0 Hz.

THEREFORE

As it was mentioned above, the maximum temperature fluctuation in hottest channel is ~ 0.09 $^{\circ}\text{C}$, therefor it is expected that fluctuation of coolant velocity would not be impressive (see figure 12 and 13). Also, in the same manner, any increase in nanofluid mass fraction will increases the stability of fluid behavior (by reduction of fluctuation amplitude).

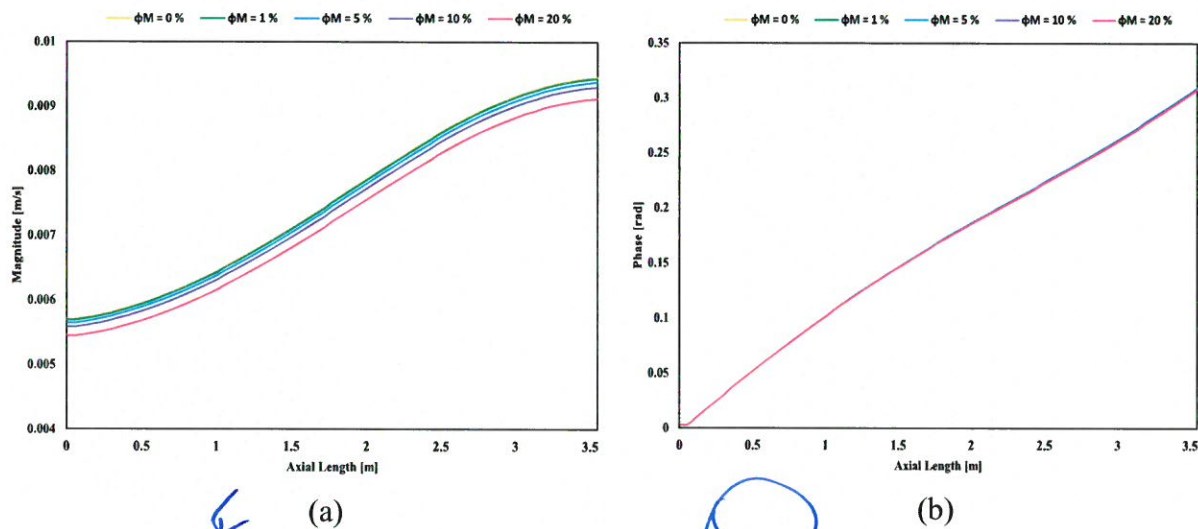


Fig. 12. F fluctuation of coolant velocity for different AL_2O_3 nanofluid mass fraction ((a) Magnitude, (b) Phase)-frequency = 0.1 Hz.

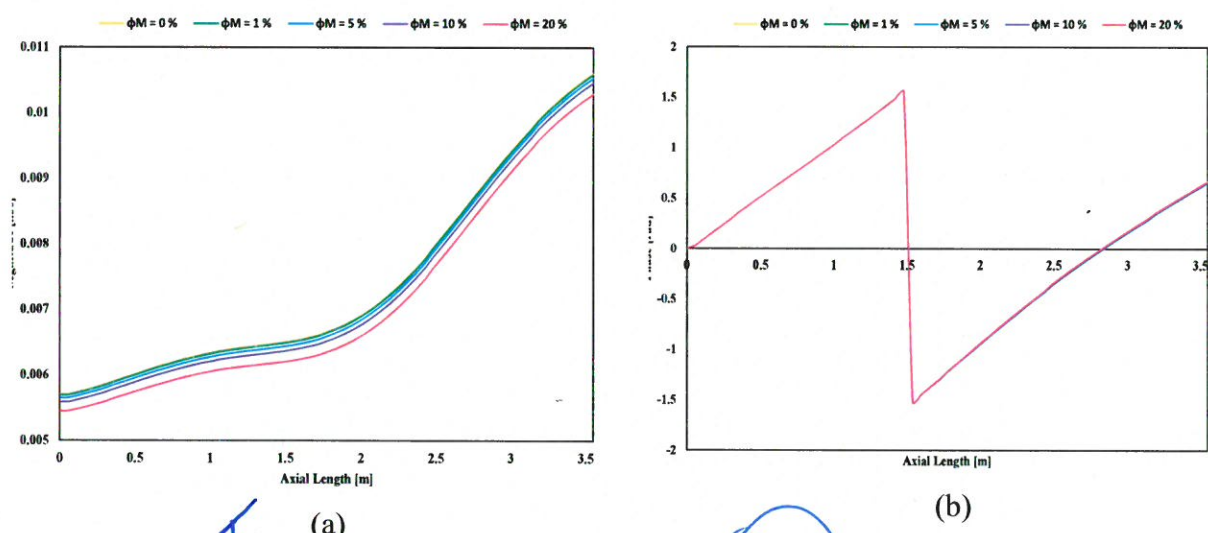


Fig. 13. F fluctuation of coolant velocity for different AL_2O_3 nanofluid mass fraction ((a) Magnitude, (b) Phase)-frequency = 1.0 Hz.

It is known that in incompressible fluids, the pressure drop in channels is mainly controlled by fluid viscosity. According to Rahimi et al., fluid viscosity will increase with increase of nanoparticles mass fraction; hence, the pressure fluctuation will linearly increase as nanoparticles increase.

CONCENTRATION

(2017)

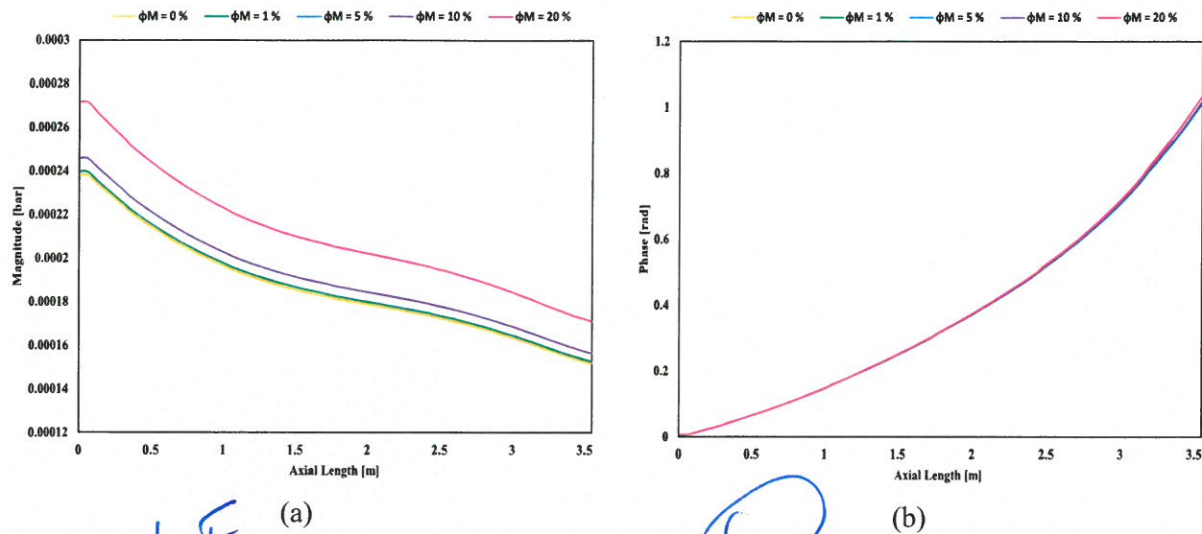


Fig. 14. F fluctuation of coolant pressure for different Al_2O_3 nanofluid mass fraction ((a) Magnitude, (b) Phase)-frequency = 0.1 Hz.

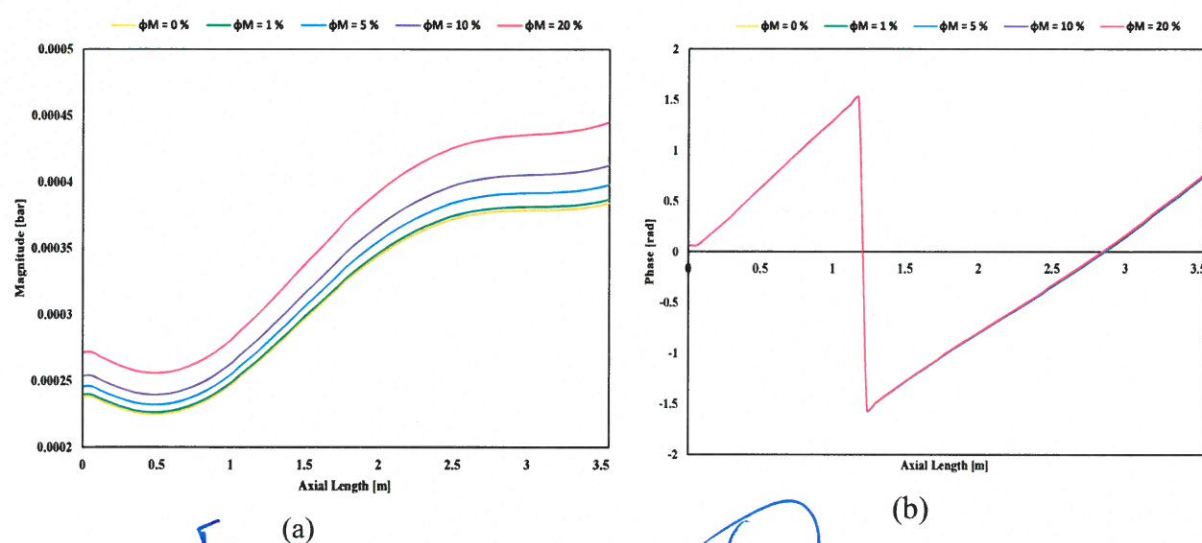


Fig. 15. F fluctuation of coolant pressure for different Al_2O_3 nanofluid mass fraction ((a) Magnitude, (b) Phase)-frequency = 1.0 Hz.

Any change in boundary conditions (coolant temperature), will propagate gradually in the fuel rod with a time delay. Figure 16 and 17 illustrate that, coolant temperature fluctuations will finally be sensed in the fuel pellet temperature. Although, the magnitude of this fluctuation is too small, but the variation of nanoparticles mass fraction is quite obvious. Figure 17 illustrates that the fuel pellet temperature will confront a perturbation when the fluctuation frequency is equal to 1.0 Hz.

↳ WHAT DO YOU MEAN?

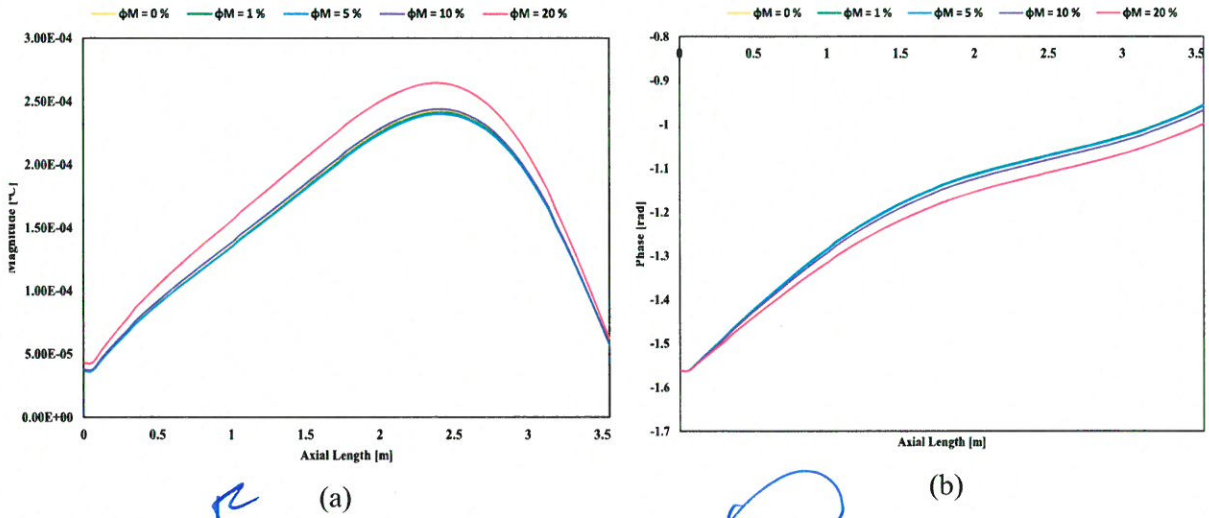


Fig. 16. Fluctuation of fuel temperature for different Al_2O_3 nanofluid mass fraction ((a) Magnitude, (b) Phase)-frequency = 0.1 Hz.

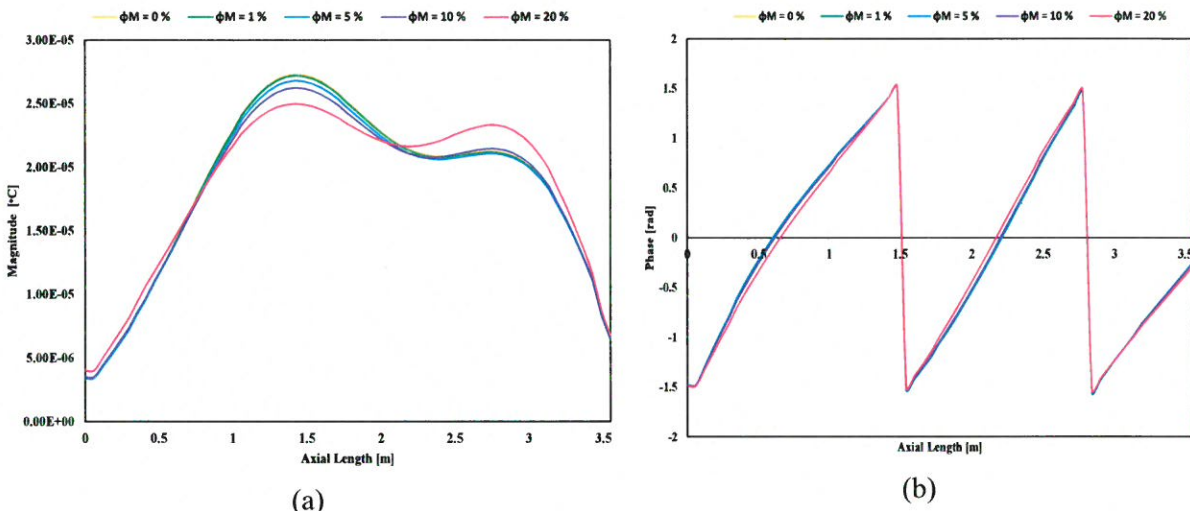


Fig. 17. Fluctuation of fuel temperature for different Al_2O_3 nanofluid mass fraction ((a) Magnitude, (b) Phase)-frequency = 1.0 Hz.

In the **second scenario**, it is assumed that the coolant inlet velocity fluctuates 0.3 m/s with the frequency equal to 0.1 Hz and 1.0 Hz.

Figure 18 and 19 illustrate the fluctuation magnitude and phase over the hottest channel in reactor core for $f = 0.1$ Hz and 1.0 Hz, respectively. In both frequencies, any increase in nanofluid mass fraction will result in increment of outlet temperature fluctuation.

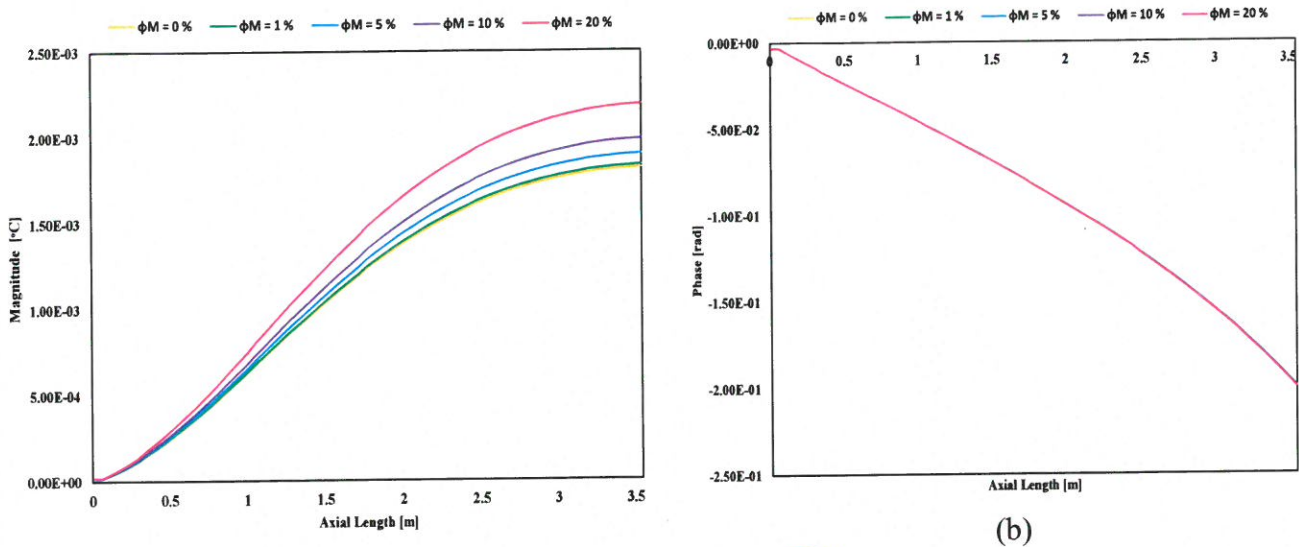


Fig. 18. Fluctuation of coolant temperature for different AL_2O_3 nanofluid mass fraction ((a) Magnitude, (b) Phase)-frequency = 0.1 Hz.

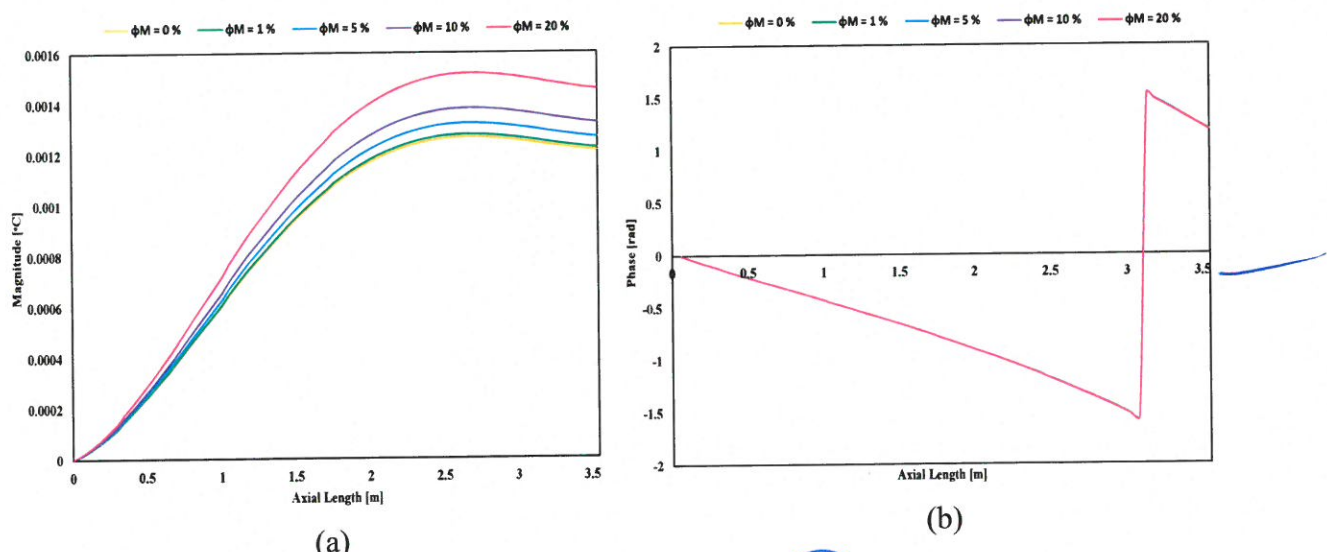


Fig. 19. Fluctuation of coolant temperature for different AL_2O_3 nanofluid mass fraction ((a) Magnitude, (b) Phase)-frequency = 1.0 Hz.

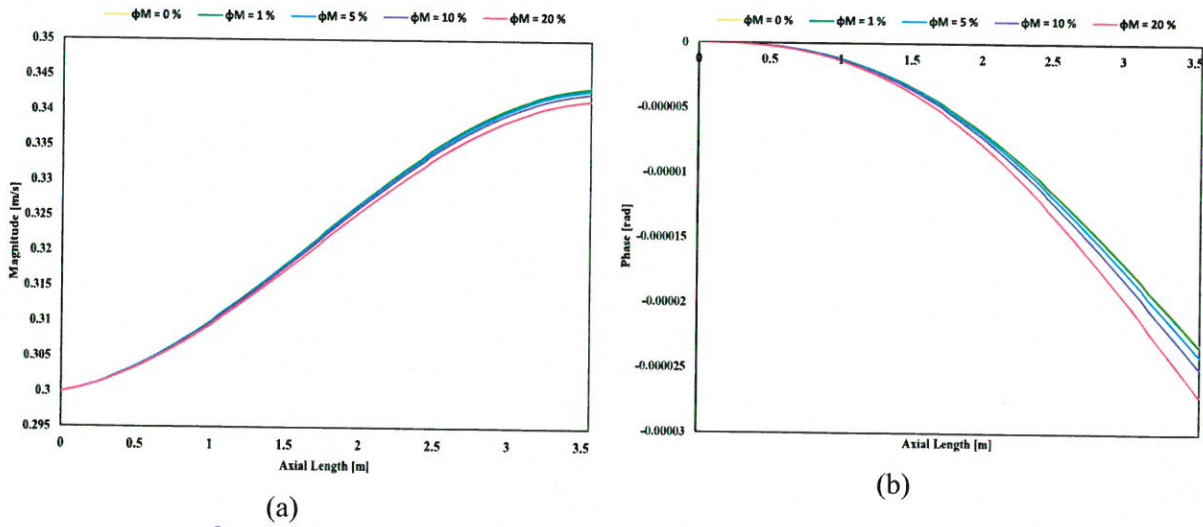


Fig. 20. Fluctuation of coolant velocity for different AL_2O_3 nanofluid mass fraction ((a) Magnitude, (b) Phase)-frequency = 0.1 Hz.

Variation of coolant velocity followed by a 0.3 m/s fluctuation is depicted in figures 20 and 21. As one can see, any change in fluctuation frequency will not affect the fluctuation magnitude and in both frequencies ($f = 0.1$ Hz as well as $f = 1.0$ Hz) reduction of nanoparticles mass fraction will increases the fluctuation magnitude.

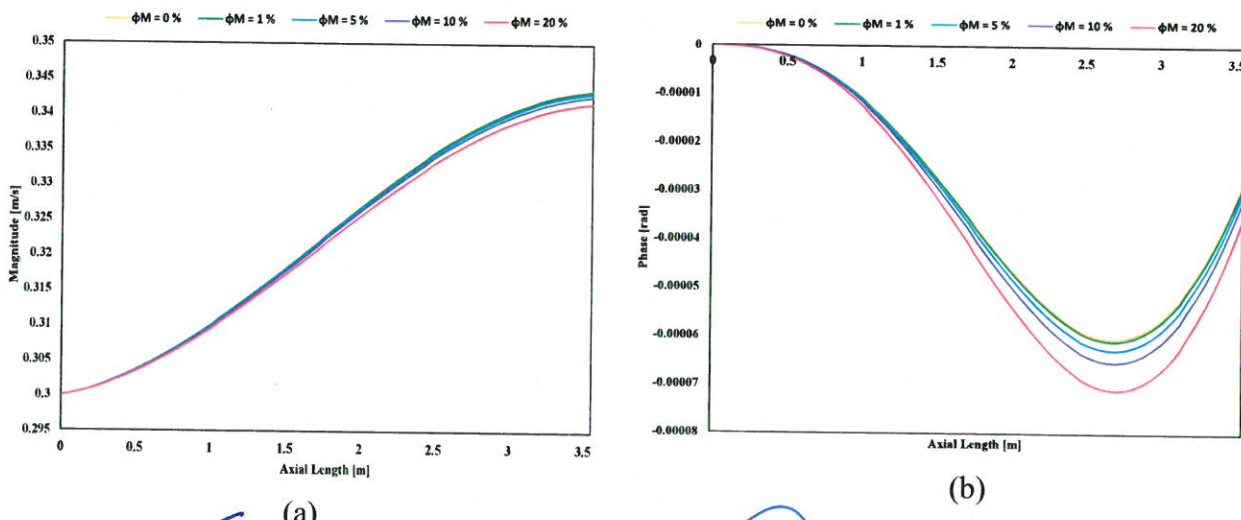


Fig. 21. Fluctuation of coolant velocity for different AL_2O_3 nanofluid mass fraction ((a) Magnitude, (b) Phase)-frequency = 1.0 Hz.

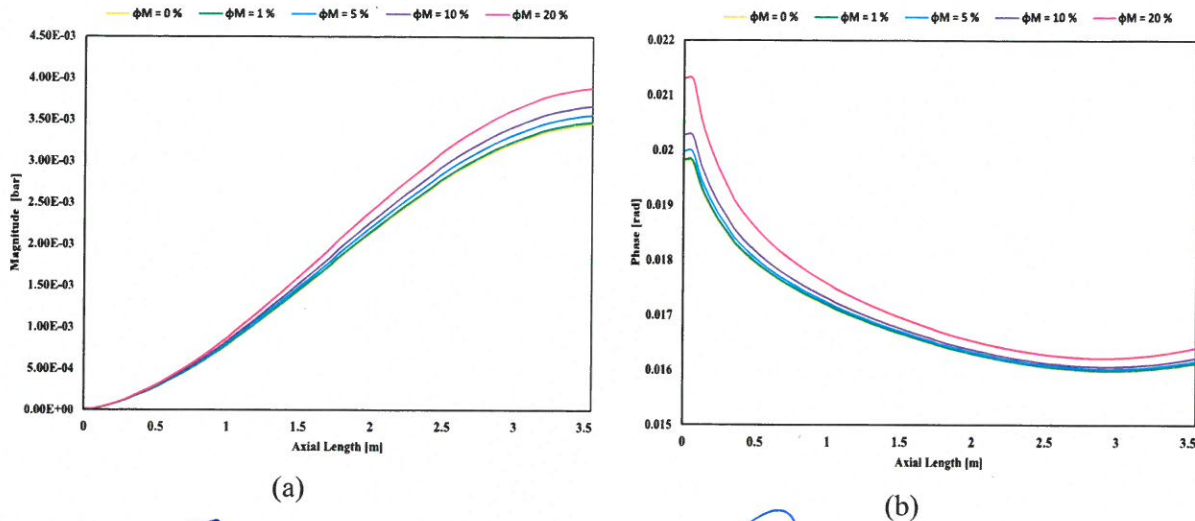


Fig. 22. F fluctuation of coolant pressure for different AL_2O_3 nanofluid mass fraction ((a) Magnitude, (b) Phase)-frequency = 0.1 Hz.

As it was mentioned earlier coolant pressure drop is a direct function of coolant viscosity which increases with nanoparticle mass fraction. Calculations show that the pressure drop magnitude is independent from fluctuation frequencies (see figure 22 and 23).

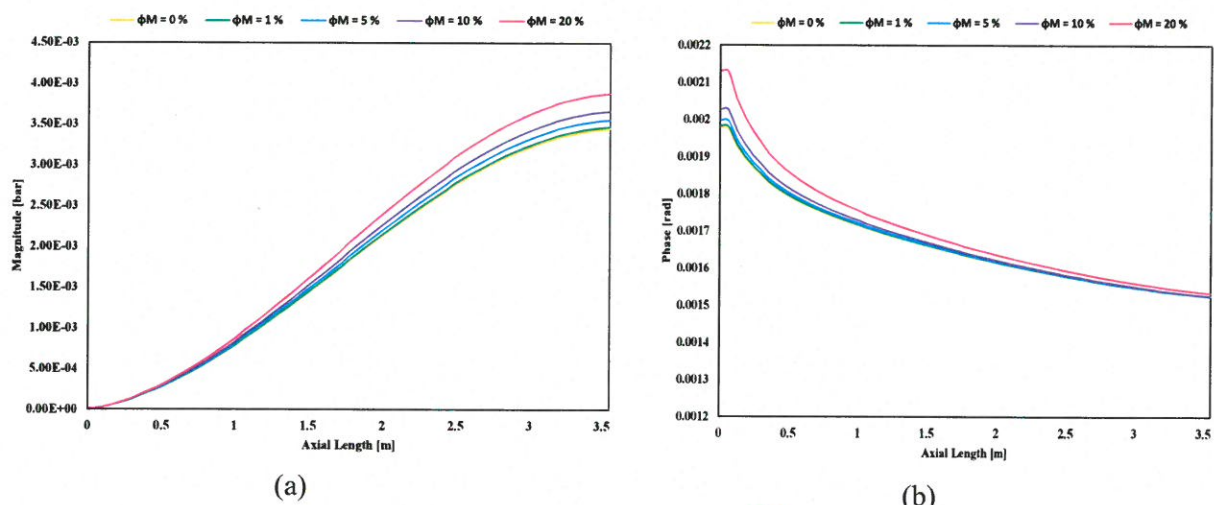


Fig. 23. F fluctuation of coolant pressure for different AL_2O_3 nanofluid mass fraction ((a) Magnitude, (b) Phase) -frequency = 1.0 Hz.

4.3 Conclusion

In the present study, a water base Al_2O_3 nanofluid was applied as coolant in a typical VVER-1000 reactor. The fluctuations in coolant temperature and velocity at the inlet of the hot fuel assembly was investigated by using conservation equations (mass, momentum and energy) in frequency space. Calculations showed that, the temperature fluctuation at coolant inlet will propagate linearly through the coolant channel and with increment in nanoparticles mass fraction the fluctuations in axial coolant temperature and velocity will be reduced. It should be noted that by increasing the fluctuation's frequency the amplification of coolant pressure, velocity and fuel temperature fluctuation are increased. In the case of a velocity fluctuation at coolant inlet, with increment of nanoparticles mass fraction the coolant temperature and pressure fluctuation magnitude will raised.

References

- AEOI, 2007. Final Safety Analysis Report (FSAR) of BNPP-1, Chapter 4 (Reactor), Revision 1. Atomic Energy Organization of Iran (AEOI), Tehran, Iran.
- Choi, S.U.S. 1995. Developments and applications of non-Newtonian flows. American Society of Mechanical Engineers, New York, 99-105.
- Gholamreza Jahanfarnia, Ehsan Zarifi, Farzad Veysi ,2013.Thermal–hydraulic modeling of nanofluids as the coolant in VVER-1000 reactor core by the porous media approach, Annals of Nuclear Energy 51, 203–212.
- J. Buongiorno, 2005. Convective Transport in Nanofluids, *Journal of Heat Transfer* 128(3), Aug 15, 240-250.
- Katona, T., Meskó, L., Pór, G., Valkó, J., 1982. Some aspects of the theory of neutron noise due to propagating disturbances. *Prog. Nucl. Energy* 9, 209–222.
- Kosály, G., Williams, M.M.R., 1971. Point theory of the neutron noise induced by inlet temperature fluctuations and random mechanical vibrations. *Atomkernenergie* 18, 203–208.
- Larsson, V., Demazière, C., 2012. A coupled neutronics/thermal–hydraulics tool for calculating fluctuations in pressurized water reactors. *Ann. Nucl. Energy* 43, 68–76.
- Malmir, H., Vosoughi, N., 2015a. Calculation and analysis of thermal-hydraulics fluctuations in pressurized water reactors. *Ann. Nucl. Energy* 76, 75–84.
- Mauro Lomascolo, Gianpiero Colangelo, Marco Milanese, Arturode Risi, 2015. Review of heat transfer in nanofluids: Conductive, convective and radiative experimental results, *Renewable and Sustainable Energy Reviews* 43, page: 1182–1198.
- Murthy, J.Y., 2002. Numerical Methods in Heat, Mass and Momentum Transfer (Lecture Notes). School of Mechanical Engineering, Purdue University, Indiana, USA.
- M. Ebrahimian, G.R. Ansarifar, 2016. Investigation of the nano fluid effects on heat transfer characteristics in nuclear reactors with dual cooled annular fuel using CFD (Computational Fluid Dynamics) modeling, *Journal of Energy* 98, page 1-14.

- 1 M.H. Rahimi, G. Jahanfarnia, 2014. Thermal-hydraulic core analysis of the VVER-1000 reactor
2 using a porous media approach, Journal of Fluids and Structures 51, page: 85–96.
3
- 4 M.H. Rahimi, G. Jahanfarnia, N. Vosoughi, October 2017. Thermal-hydraulic analysis of
5 nanofluids as the coolant in supercritical water reactors. The Journal of Supercritical Fluids,
6 Volume 128, Pages 47-56.
7
- 8 Nakamura, S., 1977. Computational Methods in Engineering and Science with Applications to
9 Fluid Dynamics and Nuclear Systems. Wiley Interscience, New York, USA.
10
- 11 N. Masoumi, N. Sohrabi and A. Behzadmehr, 2009. A new model for calculating the effective
12 viscosity of nanofluids, J Phys D Appl Phys, 42. 055501.
13
- 14 Sheng-Qi Zhou, Rui Ni, 2008. Measurement of the specific heat capacity of water-based Al₂O₃
15 nanofluid, APPLIED PHYSICS LETTERS 92, 093123.
16
- 17 Todreas, N.E., Kazimi, M.S., 2001. Nuclear Systems I & II. Taylor and Francis, New York,
18 USA.
19
- 20 Valkó, J., 1992. In-core generated temperature fluctuations and boiling detection in pressurized
21 water reactors. Ann. Nucl. Energy 19, 155–168.
22
- 23 Wagner, W., Kretzschmar, H-J., 2008. International Steam Tables, Properties of Water and
24 Steam Based on the Industrial Formulation IAPWS-IF97, Second ed. Springer-Verlag,
25 Berlin, Germany.
26

32
33
34 DIFF FORMATS FOR CITING!
35
36
37
38
39
40
41
42
43
44
45
46
47
48
49
50
51
52
53
54
55
56
57
58
59
60
61

Figures

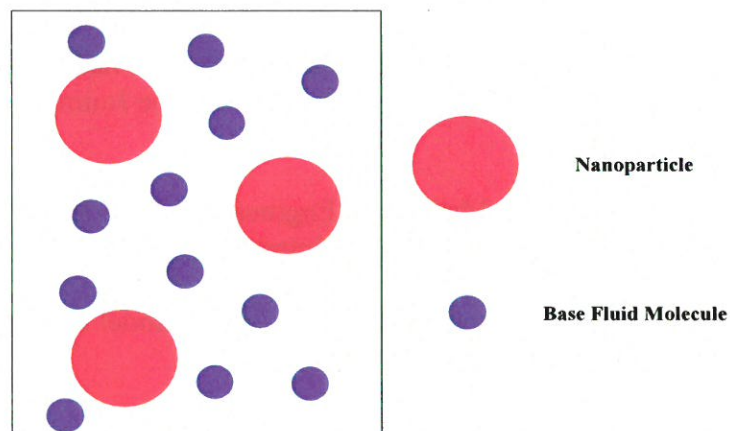


Fig. 1. Homogeneous Nanofluid in an arbitrary control volume.

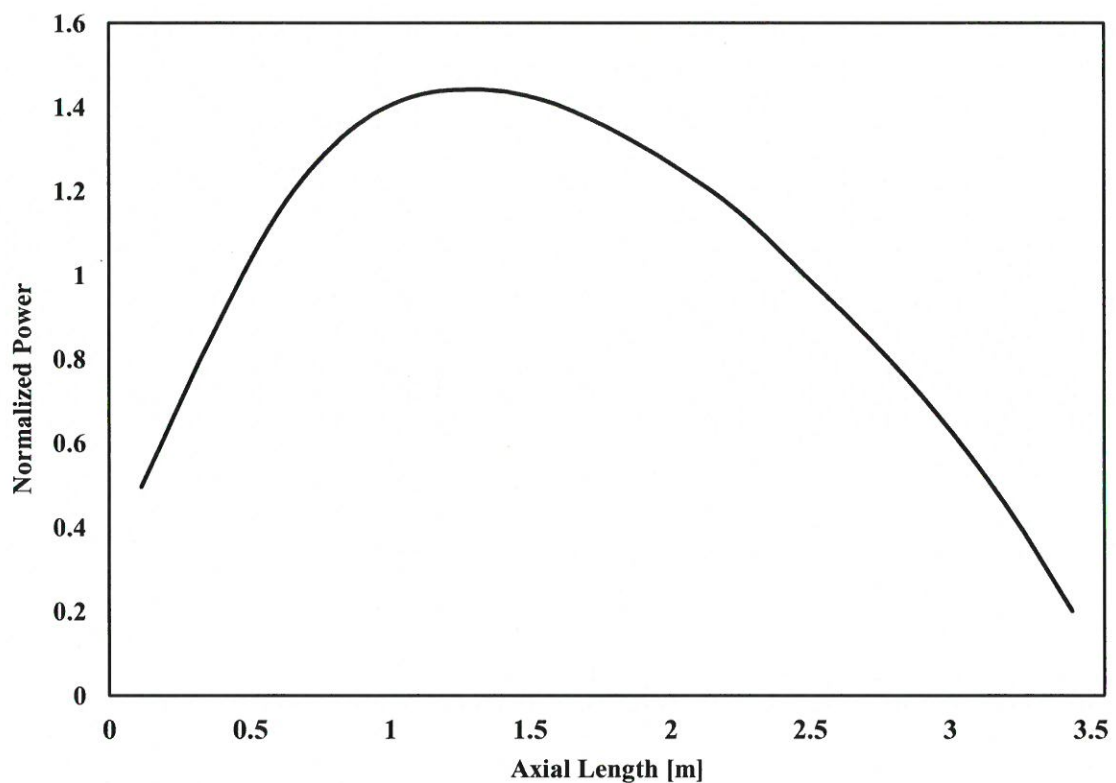


Fig. 2. Normalized axial Power distribution in the VVER-1000 reactor.